# Supporting information

## Hydrogen Spillover of $Pt_5Ru_1$ Nanoalloy Improves $Ni_3S_2$ Highly Efficient pH-universal Electrocatalytic Hydrogen Evolution

*Zuxi Yu, Xianhong Rui, Yan Yu**

Z. Yu, Prof. Y. Yu

Hefei National Research Center for Physical Sciences at the Microscale, Department of Materials Science and Engineering, CAS Key Laboratory of Materials for Energy Conversion, University of Science and Technology of China, Hefei, Anhui 230026, China. E-mail: yanyumse@ustc.edu.cn

Prof. X. Rui

School of Materials and Energy, Guangdong University of Technology, Guangzhou, 510006 China.

Prof. Y. Yu

National Synchrotron Radiation Laboratory, Hefei, Anhui 230026, China.

### Experimental Section

#### Synthesis of $Ni_3S_2$@NF

$Ni_3S_2$@NF was synthesized by one-step hydrothermal method. 16 mM $Na_2S·9H_2O$ was added to deionized water (30 mL) and stirred vigorously. Then, 4×2 $cm^2$ of washed nickel foam was placed into autoclave and heated at 120 °C for 6h. After the reaction, the sample was vacuum dried at 60 °C for 3h.

#### Synthesis of $Ni_3S_2/Pt_5Ru_1$@NF

The final $Ni_3S_2/Pt_5Ru_1$@NF sample was acquired by chemical reduction at room temperature. $H_2PtCl_6·6H_2O$ (0.575 mmol), $RuCl_3$ (0.575 mmol), and $Na_3C_6H_5O_7·2H_2O$ (0.01 M) were dissolved into deionized water (40 mL) and stirred evenly. Then, the $Ni_3S_2$@NF and $NaBH_4$ (0.01 M) were put into it. After reaction for 1 h, the obtained

$Ni_3S_2/Pt_5Ru_1$@NF was washed by deionized water and dried at 60 °C for 3 h under vacuum.

**Synthesis of $Ni_3S_2$/Pt@NF**

The $Ni_3S_2$/Pt@NF control sample was acquired by chemical reduction at room temperature. $H_2PtCl_6 \cdot 6H_2O$ (0.575 mmol), $Na_3C_6H_5O_7 \cdot 2H_2O$ (0.005 M) were dissolved into deionized water (20 mL) and stirred evenly. Then, the $Ni_3S_2$@NF and $NaBH_4$ (0.005 M) were put into it. After reaction for 1 h, the obtained $Ni_3S_2/Pt_5Ru_1$@NF was washed by deionized water and dried at 60 °C for 3 h under vacuum.

**Synthesis of $Ni_3S_2$/Ru@NF**

The $Ni_3S_2$/Ru@NF control sample was acquired by chemical reduction at room temperature. $RuCl_3$ (0.575 mmol), $Na_3C_6H_5O_7 \cdot 2H_2O$ (0.005 M) were dissolved into deionized water (20 mL) and stirred evenly. Then, the $Ni_3S_2$@NF and $NaBH_4$ (0.005 M) were put into it. After reaction for 1 h, the obtained $Ni_3S_2/Pt_5Ru_1$@NF was washed by deionized water and dried at 60 °C for 3 h under vacuum.

**Synthesis of Pt/C@NF**

Pt/C@NF was synthesis by immobilizing Pt/C onto NF. An immobilization ink solution was firstly prepared by mixing 10 mg Pt/C with 40 μL Nafion, then dispersed in 1.0 mL of water-ethanol solution ($V_{Water}$ / $V_{Ethanol}$ = 4:1), followed by 30 min sonication. A piece of the treated NF was then immersed into the ink solution for 3 min and dried in air at room temperature.

**Material Characterization**

The morphologies of $Ni_3S_2/Pt_5Ru_1$@NF, $Ni_3S_2$/Pt@NF, $Ni_3S_2$/Ru@NF, Pt/C@NF and Ni foam were observed employing field-emission scanning electron microscope (ZEISS, Gemini SEM 300) and transmission electron microscope (JEOL, 4000EX). High-resolution transmission electron microscopy (HRTEM) of the $Ni_3S_2/Pt_5Ru_1$@NF was characterized by transmission electron microscope (JEOL, 4000EX). Raman

scattering spectra were recorded by a Renishaw System 2000 spectrometer. The crystalline structures of these samples were characterized using X-ray diffraction (Rigaku, TTR-III) with a Cu Kα radiation. The chemical states of the sample on the surface were analyzed by XPS (ESCALAB 250Xi). Proportion of Ni, S, Pt and Ru in $Ni_3S_2/Pt_5Ru_1$@NF was measured by inductive coupled plasma emission spectrometer (Optima 7300 DV).

**Electrochemical Characterization**

Electrochemical measurements were achieved by Autolab electrochemical analyzer with a typical three-electrode system comprising of the $Ni_3S_2/Pt_5Ru_1$@NF sample as the working electrode, graphite rod electrode as the counter electrode and Ag/AgCl as the reference electrode. All potentials mentioned in this work were revised to reversible hydrogen electrode (RHE) by means of Nernst equation. First, cyclic voltammograms (CVs) with different rate of 20 and 100 mV $s^{-1}$ were applied to activate the working electrode. Then, the linear sweep voltammetry (LSV) curves were recorded at 5 mV $s^{-1}$ with 95% iR-corrections to remove barrier of uncompensated resistance. Electrochemical impedance spectroscopy (EIS) measurement was conducted at the amplitude voltage of 5 mV by using AC impedance technology with range from 0.1 MHz to 100 mHz. To estimate double-layer capacitance (Cdl), CV measurements were achieved by different scan rates ranging from 25 to 150 mV in the potential windows -0.98 to -0.88 V for HER. Long-term stability tests were conducted using chronopotentiometry under continuous current density. Additionally, 1.0 M KOH and 0.1 M $HClO_4$ solution was used for above electrochemical test. The TOF value is obtained by following Eq. (1):

$$TOF = \frac{J \times A}{N \times F \times n} \quad (1)$$

where J is the measured current density, A is geometric area of the electrode, N is the number of electrons required for reaction, F is Faraday constant and n is the number of active sites. The electrochemical surface area (ECSA) of $Ni_3S_2/Pt_5Ru_1$@NF and control samples were estimated from their $C_{dl}$ value. And the detailed ECSA is acquired by

ECSA = $C_{dl}/C_s$, where $C_s$ is the specific capacitance of the sample, which is usually between 20 and 60 μF $cm^{-2}$ and here we take the average value of 40 μF $cm^{-2}$ for calculation.

**Computational Methods**

All DFT calculations were accomplished by using Vienna Ab Initio Simulation Package (VASP), adopting the projector augmented wave (PAW) method.[1] The generalized gradient approximation (GGA) with Perdew-Burke-Ernzerhof (PBE) version was utilized to represent the exchange and correlation energies.[2] A cut-off kinetic energy of 520 eV was selected for plane-wave basis functions and the 3 × 3 × 1 Monkhorst–Pack grids were applied to all DFT optimizations.[3] The adjacent slabs were separated by a vacuum layer of 15 Å, which is sufficiently large to exclude the influence of models in vertical direction. In overall HER pathway, protons would be produced on the surface of electrocatalysts and the free energy of protons ($\Delta G_H$) is the key indicator to evaluate HER catalytic activity and is achieved by following Eq. (2):

$$\Delta G_H = \Delta E_H + \Delta E_{ZPE} - T\Delta S_H \quad (2)$$

where $\Delta E_H$, $\Delta E_{ZPE}$ and $T\Delta S_H$ are described the binding energy, zero-point energy change and entropy difference of hydrogen adsorption, respectively. And ΔEH is calculated by following Eq. (3):

$$\Delta E_H = E_{surf+H} - E_{surf} - 1/2E_{H2} \quad (3)$$

where the $E_{surf+H}$ is the total energy of absorbed system, the $E_{surf}$ and $E_{H2}$ are the energies of bare surface and gas phase species, respectively.

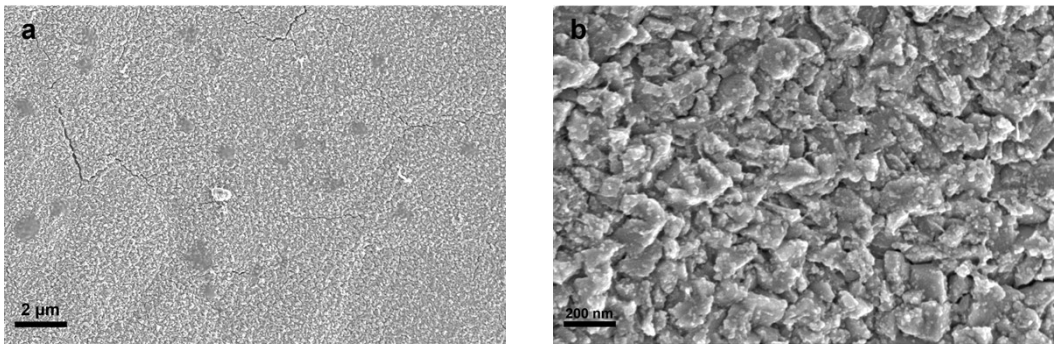


**Figure S1.** SEM images of $Ni_3S_2/Pt_5Ru_1$@NF: (a) low magnification, and (b) high magnification.

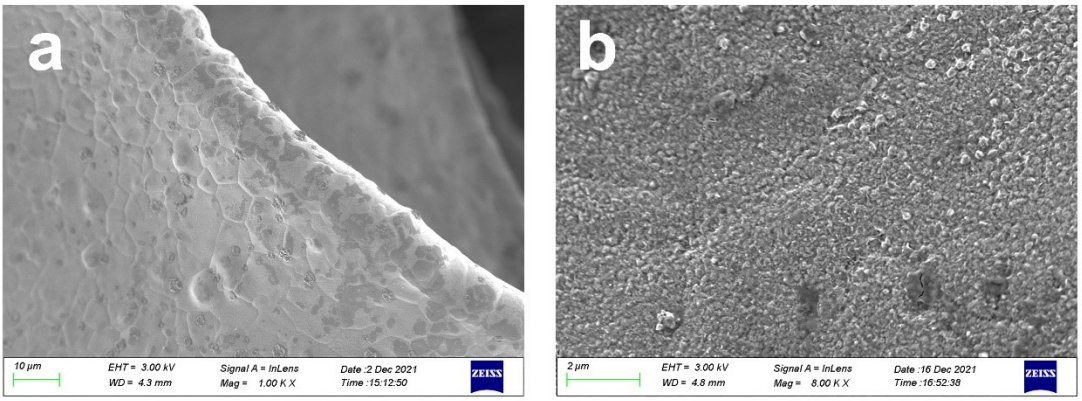


**Figure S2.** SEM photos of control samples. (a) Ni Foam, (b) $Ni_3S_2$@NF.

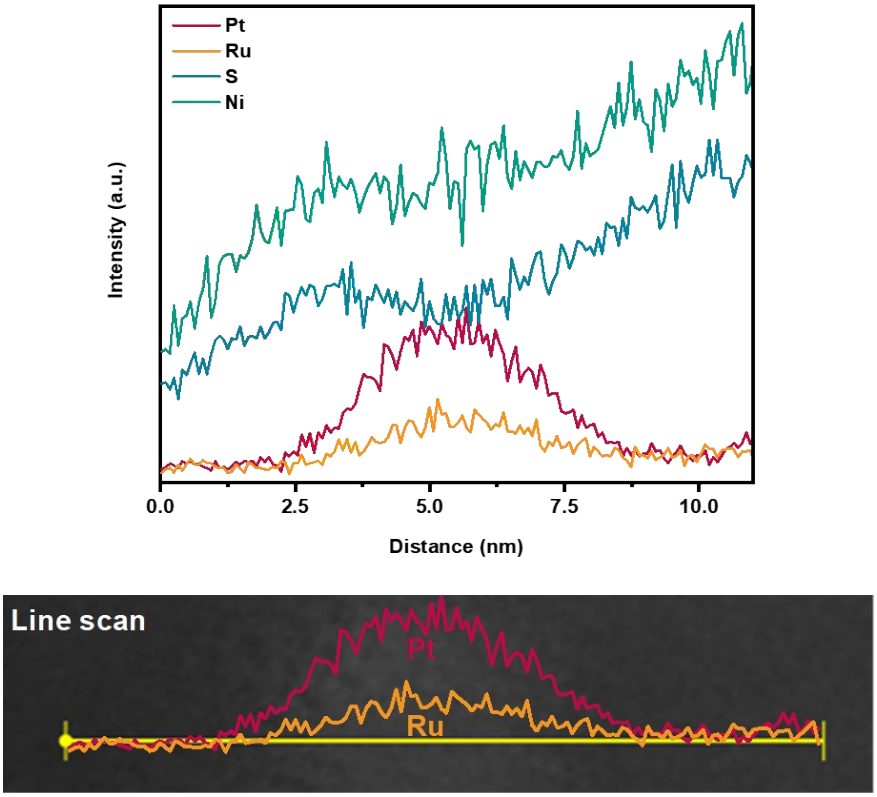


**Figure S3.** Line scan for the $Ni_3S_2/Pt_5Ru_1$@NF.

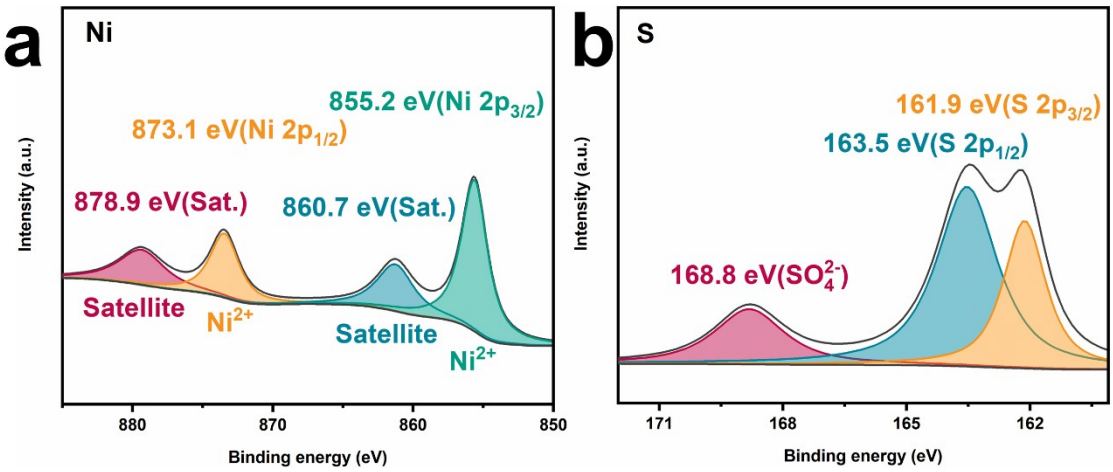


**Figure S4.** XPS spectra of (a) Ni 2p, (b) S 2p in $Ni_3S_2$@NF.

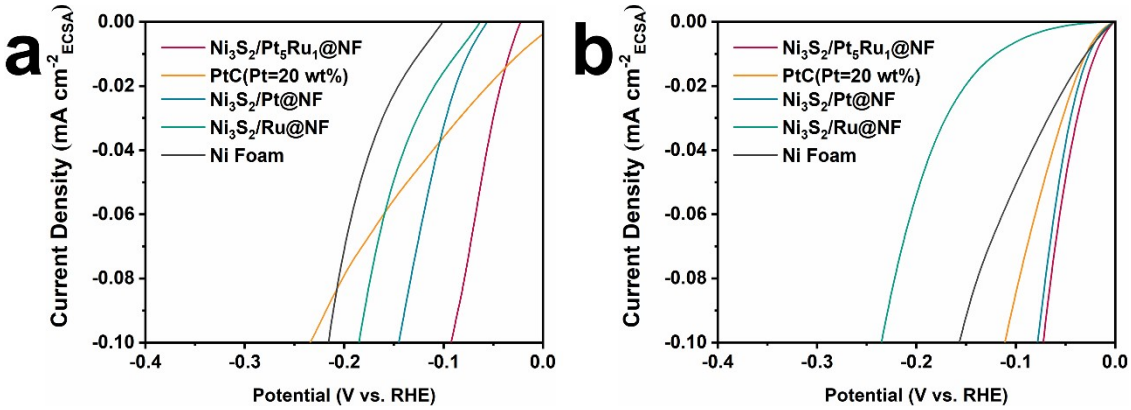


**Figure S5.** Polarization curves of $Ni_3S_2/Pt_5Ru_1$@NF and control samples based on ECSA-normalization toward HER in (a) 0.1 M $HClO_4$, (b) 1.0 M KOH.

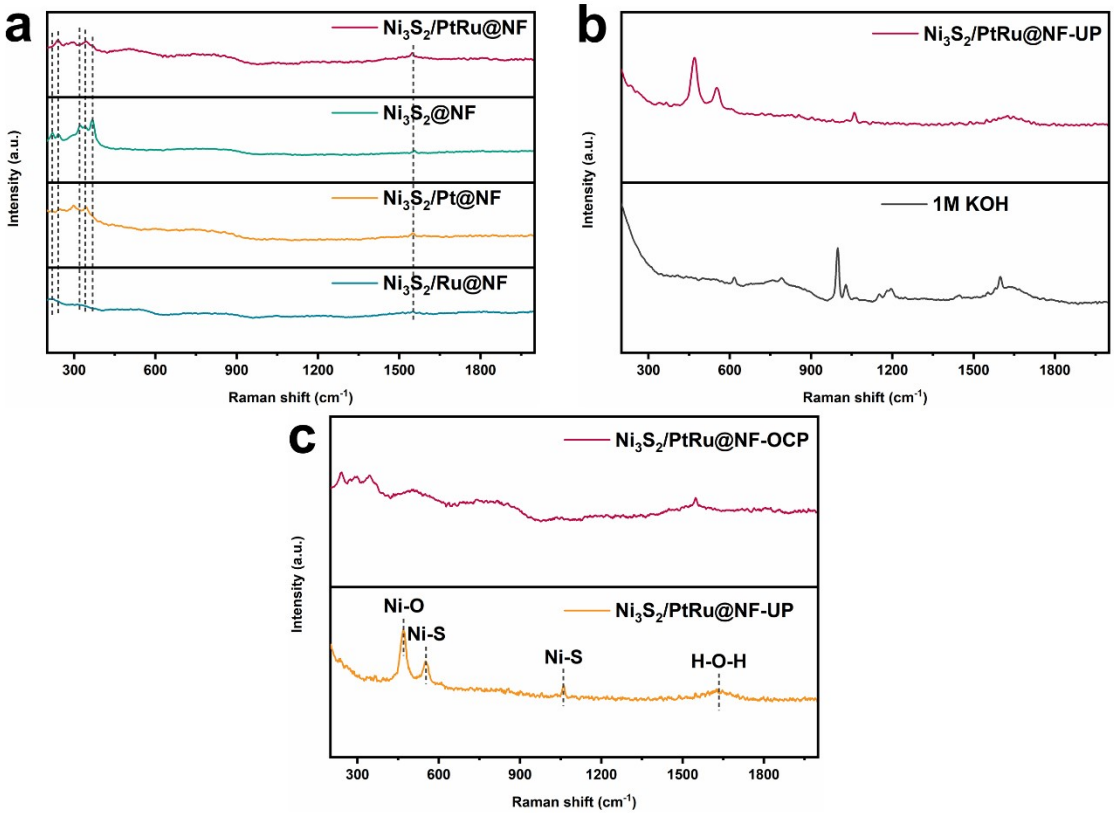


**Figure S6.** Raman spectra of $Ni_3S_2/Pt_5Ru_1$@NF and control samples. (a) Pristine states, (b) 1.0 M KOH and $Ni_3S_2/Pt_5Ru_1$@NF in 1.0 M KOH, and (c) $Ni_3S_2/Pt_5Ru_1$@NF with (up)/without 1.0 M KOH.

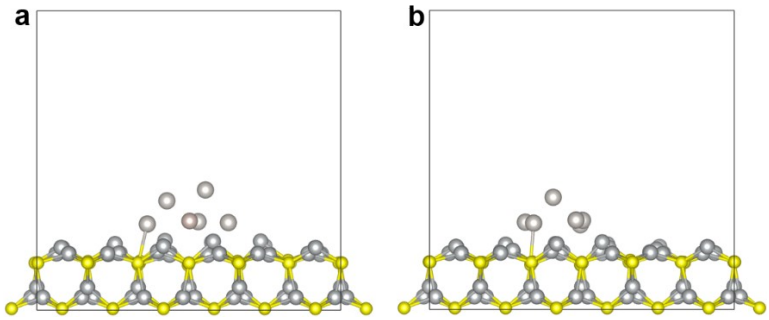


**Figure S7.** Calculated models of (a) $Ni_3S_2/Pt_5Ru_1$, and (b) $Ni_3S_2/Pt_6$.

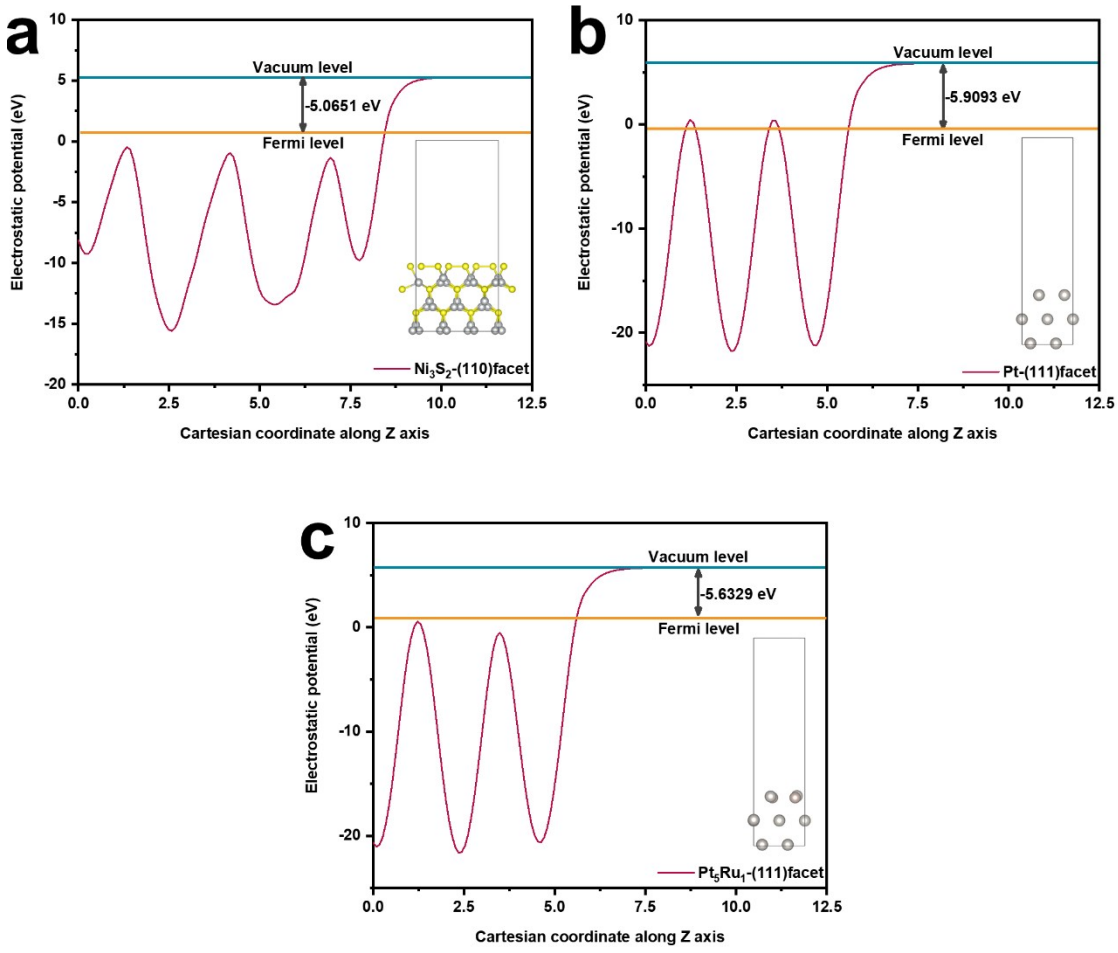


**Figure S8.** Calculated work function (ϕ) of (a) $Ni_3S_2$, (b) Pt, and (c) $Pt_5Ru_1$.

**Table S1.** ICP-MS analysis of series of $Ni_3S_2/Pt_5Ru_1$@NF catalysts.

| Catalyst | Pt loading [wt. %] | Ru loading [wt. %] | Molar ratio of Pt : Ru |
|---|---|---|---|
| $Ni_3S_2/Pt_5Ru_1$@NF | 1.52 | 0.30 | 5.07 |
| $Ni_3S_2$/Pt@NF | 1.85 | / | / |
| $Ni_3S_2$/Ru@NF | / | 1.78 | / |

**Table S2.** The fitted parameters of the EIS data of $Ni_3S_2/Pt_5Ru_1$@NF, Pt/C, $Ni_3S_2$/Pt@NF, $Ni_3S_2$/Ru@NF and Ni foam for HER in 1.0 M KOH.

| Parameter | $Ni_3S_2/Pt_5Ru_1$ @NF | Pt/C (Pt=20 %) | $Ni_3S_2$/Pt@ NF | $Ni_3S_2$/Ru @NF | Ni Foam |
|---|---|---|---|---|---|
| $R_s$ | 0.69683 | 0.72489 | 0.70316 | 0.70271 | 0.67703 |
| T-T | 0.31780 | 0.00149 | 0.30957 | 0.00830 | 0.00202 |
| T-P | 0.71219 | 0.81157 | 0.70055 | 0.86512 | 0.78460 |
| $R_1$ | 6.53500 | 20.39000 | 8.16600 | 48.55000 | 21.53000 |
| $C_\psi$ | 0.92857 | 0.00002 | 0.00428 | 0.00334 | 0.00001 |
| $R_2$ | 4.90600 | 25.39000 | 11.38000 | 46.27000 | 28.19000 |

**Table S3.** The fitted parameters of the EIS data of $Ni_3S_2/Pt_5Ru_1$@NF, Pt/C, $Ni_3S_2$/Pt@NF, $Ni_3S_2$/Ru@NF and Ni foam for HER in 0.1 M $HClO_4$.

| Parameter | $Ni_3S_2/Pt_5Ru_1$ @NF | Pt/C (Pt=20 %) | $Ni_3S_2$/Pt @NF | $Ni_3S_2$/Ru @NF | Ni Foam |
|---|---|---|---|---|---|
| $R_s$ | 5.71300 | 5.43700 | 5.74000 | 5.77900 | 5.54700 |
| T-T | 0.02815 | 0.00129 | 0.03998 | 0.00656 | 0.00039 |
| T-P | 0.52085 | 0.69569 | 0.60584 | 0.83801 | 0.85548 |
| $R_1$ | 0.69609 | 3.84400 | 0.52661 | 2.49700 | 3.67700 |
| $C_\psi$ | 0.00347 | 0.51852 | 0.00139 | 0.00271 | 0.00007 |
| $R_2$ | 5.73700 | 7.17800 | 5.93600 | 3.43900 | 13.94000 |

**Table S4.** Comparison of electrochemical performance of $Ni_3S_2/Pt_5Ru_1$@NF catalyst with other reported nickel-based chalcogenides catalysts.

| Catalysts | η@10 mA $cm^{-2}$ mV | Tafel slope mV $dec^{-1}$ | Electrolyte (KOH) | Substrate | Ref. |
|---|---|---|---|---|---|
| $Ni_3S_2/Pt_5Ru_1$@NF | 13 | 62.4 | 1.0 | NF | This work |
| $Ni_3S_2$ | 186 | 89.3 | 1.0 | NF | [4] |
| $Ni_3S_2$/MnS-O | 116 | 41 | 1.0 | NF | [5] |
| $CoNi_2S_4/Ni_3S_2$ | 171 | 88.6 | 1.0 | NF | [6] |
| δ-FeOOH/$Ni_3S_2$ | 106 | 82.6 | 1.0 | NF | [7] |
| $NiWO_4$-$Ni_3S_2$ | 136 | 112 | 1.0 | NF | [8] |
| Fe-Mo-S/$Ni_3S_2$ | 141 | 123 | 1.0 | NF | [9] |
| $Co_3O_4$@Mo-$Co_3S_4$-$Ni_3S_2$ | 116 | 98 | 1.0 | NF | [10] |
| $Ni_3S_2/MnO_2$ | 102 | 69 | 1.0 | NF | [11] |
| $MoS_2/Co_9S_8/Ni_3S_2$ | 113 | 85 | 1.0 | NF | [12] |
| $Ni_3S_2$@NiV-LDH | 126 | 90 | 1.0 | NF | [13] |

**References**


[1] G. Kresse, J. J. C. m. s. Furthmüller, **1996**, 6, 15.

[2] J. P. Perdew, K. Burke, M. J. P. r. l. Ernzerhof, **1996**, 77, 3865.

[3] H. J. Monkhorst, J. D. Pack, *Phys. Rev. B* **1976**, 13, 5188.

[4] L. Li, C. Sun, B. Shang, Q. Li, J. Lei, N. Li, F. Pan, *J. Mater. Chem. A* 7 (**2019**) 18003-18011.

[5] Y. Zhang, J. Fu, H. Zhao, R. Jiang, F. Tian, R. Zhang, *Appl. Catal. B-Environ*. 257 (**2019**) 117899.

[6] W. Dai, K. Ren, Y. A. Zhu, Y. Pan, J. Yu, T. Lu, *J. Alloys Compd*. 844 (**2020**) 156252.

[7] X. Ji, C. Cheng, Z. Zang, L. Li, X. Li, Y. Cheng, X. Yang, X. Yu, Z. Lu, X. Zhang, H. Liu, *J. Mater. Chem. A* 8 (**2020**) 21199-21207.

[8] S. Huang, Y. Meng, Y. Cao, F. Yao, Z. He, X. Wang, H. Pan, M. Wu, *Appl. Catal. B-Environ*. 274 (**2020**) 119120.

[9] Y. Zhang, H. Guo, X. Li, J. Du, W. Ren, R. Song, *Chem. Eng. J*. 404 (**2020**) 126483.

[10] Q. Wu, A. Dong, C. Yang, L. Ye, L. Zhao, Q. Jiang, *Chem. Eng. J*. 413 (**2021**) 127482.

[11] Y. Xiong, L. Xu, C. Jin, Q. Sun, *Appl. Catal. B-Environ*. 254 (**2019**) 329-338.

[12] Y. Yang, H. Yao, Z. Yu, S. M. Islam, H. He, M. Yuan, Y. Yue, K. Xu, W. Hao, G. Sun, H. Li, S. Ma, P. Zapol, M. G. Kanatzidis, *J. Am. Chem. Soc*. 141 (**2019**) 10417-10430.

[13] Q. Liu, J. Huang, Y. Zhao, L. Cao, K. Li, N. Zhang, D. Yang, L. Feng, L. Feng, *Nanoscale* 11 (**2019**) 8855-8863.